Surface & Coatings Technology 202 (2008) 5319–5324

Contents lists available at ScienceDirect

Surface & Coatings Technology

journal homepage: www.elsevier.com/locate/surfcoat

Sculpting on polymers using focused ion beam

M.-W. Moon [a], E.-K. Her [b], K.H. Oh [b], K.-R. Lee [a], A. Vaziri [c,*]

[a] Future Fusion Technology Research Laboratory, Korea Institute of Science and Technology, P.O. Box 131, Cheongryang, Seoul 130-650, Republic of Korea
[b] Department of Materials Science and Engineering, Seoul National University, San 56-1 Shillim, Kwanak, Seoul, 151-744, Republic of Korea
[c] Department of Mechanical and Industrial Engineering, Northeastern University, Boston, MA 02115, USA

ARTICLE INFO

Available online 13 June 2008

PACS:
62.20.mq
68.55.am
81.15.Jj

Keywords:
Focused ion beam
Polymer
Wrinkling
Dwell time
Surface modification

ABSTRACT

It has been recently shown that ordered wrinkles can be created on the surface of polymers using focused ion beam irradiation. Here, we provide an overview of the techniques developed for controlled creation of nanoscale wrinkling patterns on the polymer surface using focused ion beam. Moreover, some of the key experimental challenges for precise fabrication of wrinkling patterns were investigated by exploring the role of pixel dwell time and fluence on the morphology of the created patterns. It was demonstrated that precise modification of the polymeric surface can be achieved with high pixel dwell time at low ion fluence.

1. Introduction

The attempt to develop surface engineering techniques for polymers has yielded various methods from lithography and plasma and UVO treatment [1–5] to liquid polymer films dewetting [6,7] and thin metal film deposition on polymers [8–10]. These techniques are employed to create variety of patterns, such as dots, network structures, complex hierarchically assembled patterns, honeycomb-like structures and ring-like patterns on the surface of polymers [3–11]. On the other hand in our recent experiments with poly-dimethylsiloxane (PDMS), we have shown that focused ion beam (FIB) irradiation can be used for creation of ordered wrinkle patterns on the polymer surface [11,12]. The flexibility provided by this technique provides new avenues for creation of structural features at micron and submicron scales on the surface of polymers. The precise mechanisms underlying formation of these wrinkling patterns are not completely understood. However, it was shown that FIB irradiation results in formation of a stiff skin on the surface of PDMS, as also seen in previous experiments on the effect of ion beam irradiation on metallic surfaces [13–17]. This thin stiff skin created on the PDMS surface resembles amorphous silica [18,19] or amorphous carbon [20]. This thin stiff skin undergoes in-plane compression upon formation and buckles leading to creation of ordered wrinkles. The wavelength and morphology of the induced undulations can be effectively selected by controlling the accelerating voltage and fluence or current of the ion beam.

Surface modification by ion bombardment has been previously investigated for glassy metals [13,21], as well as amorphous [14,16,22–25] and crystalline materials [26–29]. Generally, Irradiation of ion beam normal to the surface leads to surface milling — as also seen in our recent experiments on polyimide, a polymer much stiffer that PDMS [30]. In these experiments, the ion effect is characterized by the mean penetration depth and longitudinal and lateral straggling widths [22–24]. On the other hand, ion beam irradiation at non-normal incident angle leads to appearance of features as also seen for polyimide, where surface riiples manifest [30].

These experiments suggest that FIB irradiation is a robust technique for surface engineering of polymers and can be used in an array of multi-disciplinary fields from medicine to engineering. Examples are designing biointerfaces for tissue engineering and regenerative medicine, microfluidics, biosensors and optics [3–5,31,32]. To extend the capabilities of this technique, we have developed three different methods as shown in Fig. 1. The area exposed to the ion beam can be selected by controlling the relative movement of the ion beam and polymeric substrate, or for applications that need very precise control over the exposed area by maskless patterning method.

In this paper, we complement our previous studies on controlled creation of wrinkle pattern on the polymer surface using FIB by systematically exploring the role of ion beam dwell time and ion fluence [27,33,34]. In these experiments, flat polymeric substrates were subject to ion beam irradiation with various dwell times, while

* Corresponding author.
E-mail address: vaziri@coe.neu.edu (A. Vaziri).

0257-8972/$ – see front matter © 2008 Elsevier B.V. All rights reserved.
doi:10.1016/j.surfcoat.2008.06.059

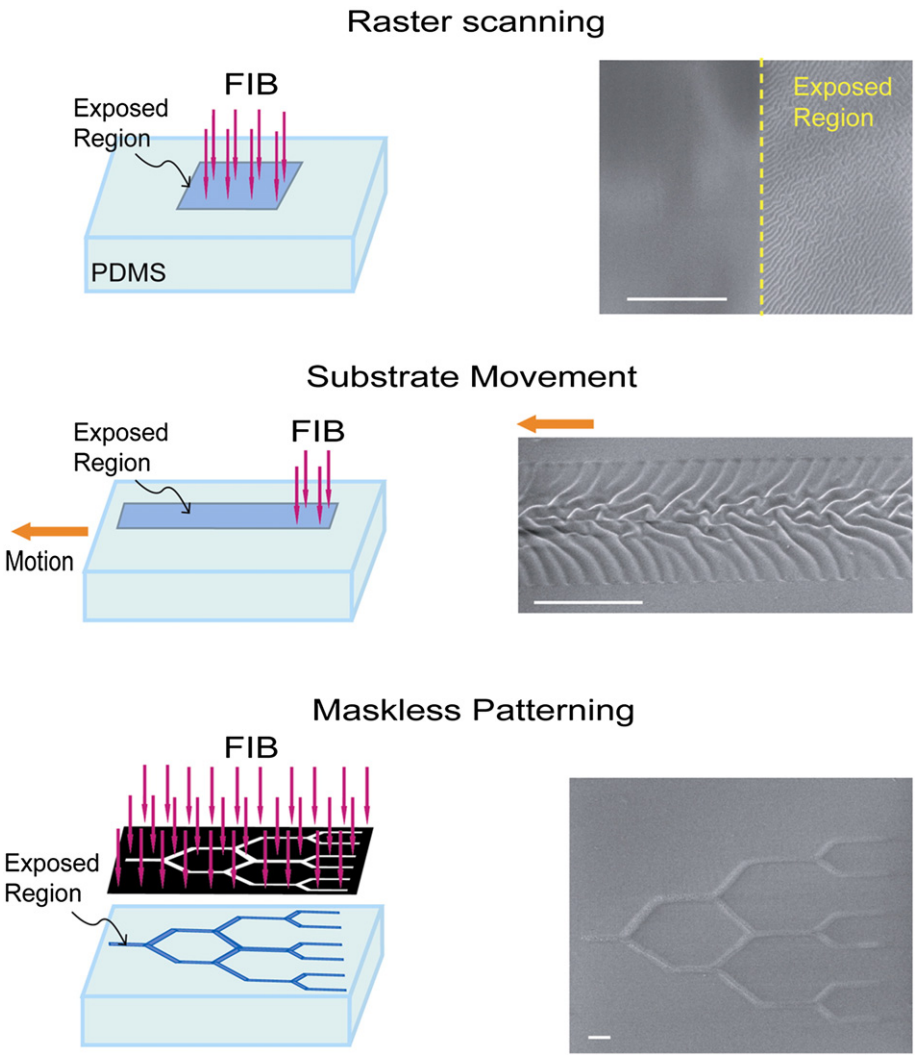

Fig. 1. Surface modification of polymers by focused ion beam. The figure displays the three methods developed for controlled creation of wrinkling patterns on desired surface areas of the polymer. The methods are shown schematically on the left, while an example of the created wrinkles for each method is shown on the right. Scale bars=10 μm.

the formation of wrinkling patterns was monitored as a function of irradiation duration and therefore ion fluence. Maskless patterning was used to create the wrinkling patterns on pre-defined complex regions of the polymeric substrate.

2. Experimental details

PDMS samples were prepared by a mixture of elastomer and cross-linker in mass ratio of 10:1 (Sylgard-184, Dow Corning, MI). The

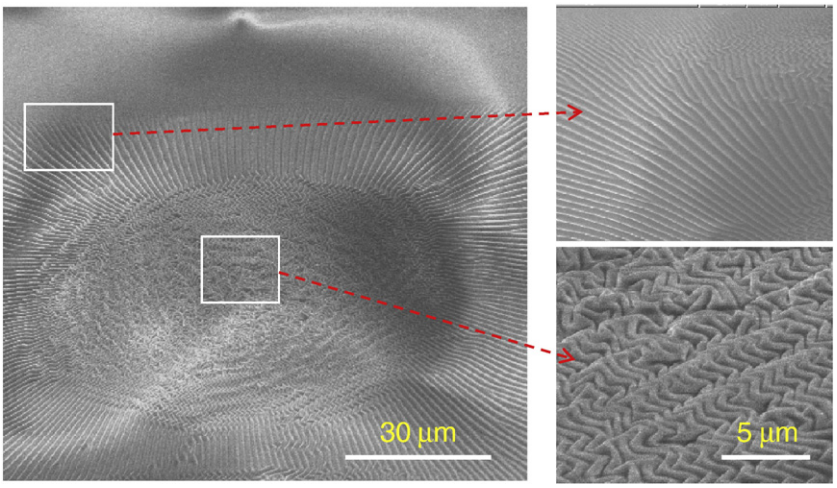

Fig. 2. SEM image of a wrinkling pattern created by focused ion beam on the PDMS surface. Approximately straight wrinkles were formed near the edges of the exposed area, while herringbone wrinkles were formed at the center of the exposed region. The ion beam had the acceleration voltage, dwell time and fluence 30 keV, 0.3 μs and 2.5×10^{13} ions/cm^2, respectively.

mixture was placed in a plastic box and stirred to remove trapped air bubbles and then cured at 80 °C for 2 hours, resulting in a cross-linked PDMS network, which was cut as coupons of dimension 20 mm×20 mm×3 mm for the experiments. A high resolution FE-SEM/FIB dual beam system (FE-SEM/FIB Dual Beam NOVA, FEI, OR) was employed for the Ga+ focused ion beam irradiation. PDMS coupons were placed in the high vacuum chamber under a working pressure of ~5×10^{-5} Pa. The PDMS surface was exposed to FIB in a digital mode with acceleration voltages of 20 and 30 keV and ion current in the range of 1 pA to 20 nA. The incident angle defined as the angle between the incoming beam and the surface normal was maintained at 0°. The pixel dwell time was varied between 500 ns and 50 μs.

The maskless patterning method of the FIB equipment was adopted for surface modification in the form of pre-defined shapes [12]. This method permits accurate selection of the areas exposed to the FIB. Bitmap files of the patterns, such as those shown as insets in Figs. 4a, 5a and 5b, were imported as a virtual mask in the focused ion beam system. The polymer surface was exposed to Ga+ ion beam with the dwell time in the range of 500 ns to 50 μs. As rectangular areas were exposed to Ga+ ion beam (digital raster mode), dwell time for each ion beam spot was varied from 500 ns to 50 μs on the scanning area.

The SEM images in the exposed region were acquired using a built-in secondary electron microscopy of the FE-SEM/FIB system. In order to suppress the electron charging phenomenon for SEM imaging, a 5 nm layer of gold was deposited along the edge of PDMS prior to FIB irradiation.

3. Results and discussion

Fig. 2 shows a wrinkling pattern created by FIB irradiation on the surface of PDMS. The morphology of the wrinkle patterns are governed by the stress state in the stiff skin induced by FIB irradiation. In Fig. 2, straight wrinkles appear near the edge of the exposed region since the stress state is almost uniaxial. In contrast, herringbone wrinkles appear close to the center of the exposed area, indicating that the stress induced in the stiff skin is approximately equi-biaxial [35]. The thickness of the stiff skin induced by FIB irradiation on the polymeric surface does not strongly depend on the ion fluence and is rather governed by the acceleration voltage of the ion beam [11,12,15]. On the other hand, the ion fluence governs the morphology of the wrinkle patterns due to its direct correlation with the induced strain in the stiff skin [11]. The critical strain associated with onset of instability in a stiff skin layer attached to a compliant substrate, ε_c, is approximately, $\varepsilon_c \approx 0.52(E_s/E_f)^{2/3}$, where E_s and E_f are the elastic moduli of the substrate and stiff skin layer, respectively [12–14,35]. Furthermore, the wavelength of the primary wrinkles, λ, of a stiff skin with thickness t, is approximately, $\lambda/t \approx 4(E_f/E_s)^{1/3}$. For the ion beam irradiation with acceleration voltage of 30 keV, substitution of $\varepsilon_c = 0.031$ and $\lambda_1 = 460$ nm from our measurement yields: $t \approx 28$ nm, $E_f/E_s \approx 70$ [11]. As acceleration voltage decreased from 30 to 5 keV, the thickness of the induced stiff skin were reduced from 28 to 5 nm and the wrinkle wavelength from 450 to 50 nm, respectively [12].

In literatures, pixel dwell time of ion beam is considered as one of the key factors that determine the accuracy of surface modification by ion beam. The dwell time controls the ion beam broadening and ion beam shifting as shown before for experiments on semiconductors [27,33,34]. In Fig. 3, we explored the role of ion beam dwell time on the wrinkle patterns created on the surface of PDMS using focused ion beam irradiation. In this set of experiment, the accelerating voltage and ion current were 30 kV and 50pA, respectively. The SEM figures display the wrinkle patterns created after 2 s of FIB irradiation, or equivalently at the ion fluence of ~1.85×10^{13} ions/cm^2. The dwell time was 0.5 μs, and 5 μs in Fig. 3b, c, respectively. For the dwell time of 0.5 μs, straight wrinkles appear at the edge of the exposed region which evolves to herringbone patterns with wavelength of ~350 μm by moving towards the center of the exposed region. For the dwell time of 5 μs, well-defined herringbone wrinkles were fabricated on the entire area exposed to the ion beam. In Fig. 3a, the boundaries of the region exposed to ion beam are not very distinct due to ion beam shifting during the repetitive scanning. However, by increasing the dwell time, this effect diminishes as a longer dwell time leads to less number of repetitive scanning at a constant fluence. Long term ion beam irradiation may lead to overflow of ion dose or ion shifting outside the patterned region due to increasing the positive ion charging effect on the surface. This effect is well-known for non-conductive materials, especially polymers, subject to ion beam irradiation [36,37]. A complementary set of experiments were carried out where wrinkle patterns were created along parallel lines by

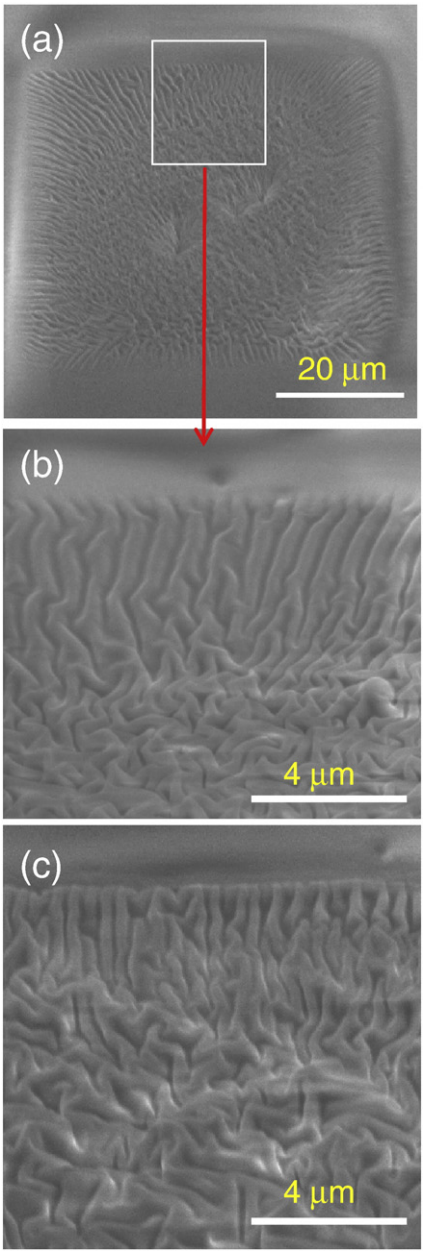

Fig. 3. Role of pixel dwell time on the morphology of patterns created by focused ion beam. (a), (b) Wrinkle pattern created at the pixel dwell time 0.5 μs. (c) The edge of the region exposed to focused ion beam with the pixel dwell time 5 μs. The ion beam accelerating voltage and density were 20 keV and 37 pA, respectively. The wrinkle patterns were created by 2s FIB irradiation, leading to the ion fluence ~1.85×10^{13} ions/cm^2.

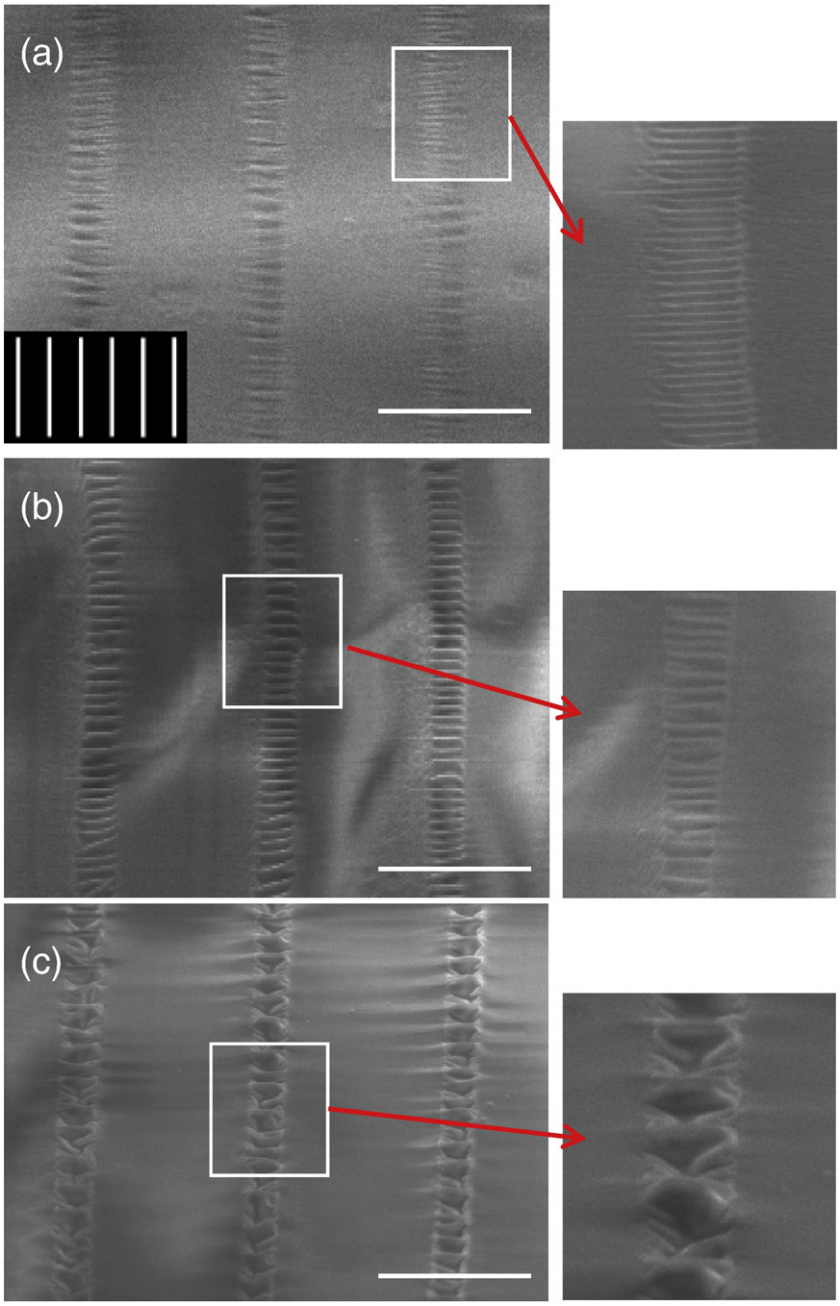

Fig. 4. Wrinkle patterns guided by maskless patterning. The pixel dwell time of the focused ion beam is 0.5, 5 and 50 μs in (a), (b) and (c), respectively. Each line has the width 2.5 μm in the bitmap file imported to as the maskless pattern. The panels on the right are magnified from the left side images. The accelerating voltage and current of ion beam were 20 keV and 0.21 nA, respectively. The ion fluence in the exposed region (denoted by white color in the inset of (a)) was ~4.0×10^{12} ions/cm^2. Scale bars = 10 μm.

employing the maskless patterning method, Fig. 4. The fluence and accelerating voltage were ~4.0×10^{12} ions/cm^2 and 20 keV, respectively. Again, shorter dwell time leads to ion beam shifting across the boundaries of confined area mainly due to a large astigmatism and defocusing caused by positive ion charging form the polymer surface. The wrinkling pattern created in Fig. 4a with the dwell time of 0.5 μs, has the average width of ~3 μm, which is larger than the width of 2.5 μm, pre-defined in the bitmap image. By increasing the dwell time to 50 μs in Fig. 4c, the wrinkles formed only on the areas guided by the bitmap image with very distinct boundaries.

In addition to the pixel dwell time, the ion fluence is considered as one of the main factors that increase the ion beam broadening and shifting during the irradiation experiment. In Fig. 5, we used maskless patterning method to study the role of ion fluence on creation of wrinkles patterns by FIB. The insets to the top figures display the bitmap image imported to the FIB system. The accelerating voltage and current of ion beam were 30 keV and 50 pA, respectively in both experiments. By adopting the circular patterns (left panel, Fig. 5a), islands of buckled stiff skins on the PDMS was created at the fluence of 2.74×10^{12} ions/cm^2. Each island had the diameter of 1.4 μm and the spacing between the islands was set as 4.2 μm. By increasing the fluence, arrays of buckled lines appear on the surface of the polymer along the rastering direction of the ion beam (left to right). At the ion fluence of 1.37×10^{13} ions/cm^2, the entire region were affected by ion beam irradiation. The reason for this alteration in the morphology of created patterns is ion beam broadening during irradiation of Ga+ ion beam, which causes the large areas of the polymeric surface to be affected by the repetitive

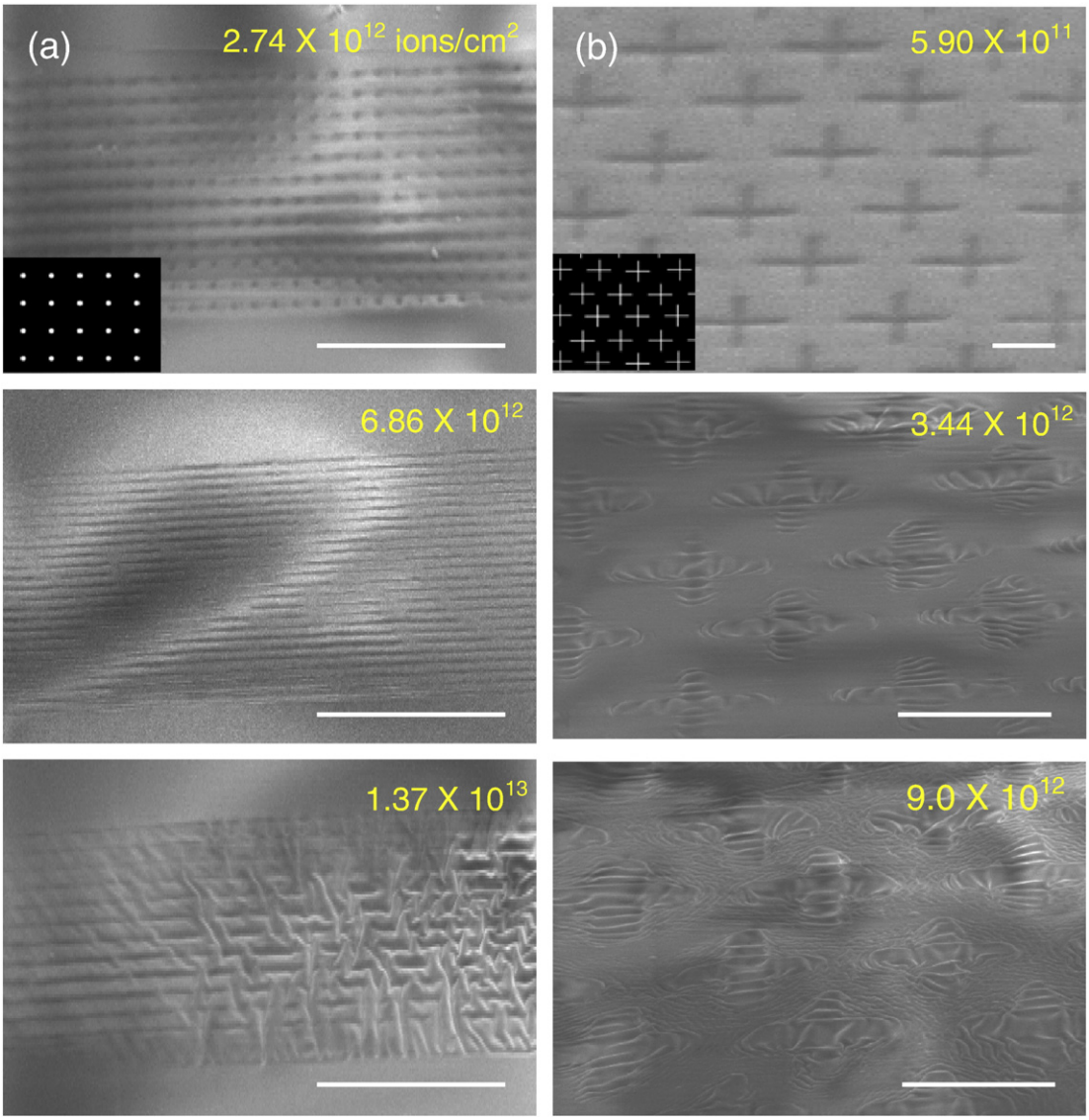

Fig. 5. Patterns created at different ion fluences by maskless patterning. Bitmap files of the patterns used are shown as insets in the top figures. The accelerating voltage and pixel dwell time were 30 keV and 50 μs, respectively. The ion fluence for each wrinkling patterns is shown in the figures. Scale bars = 10 μm.

rastering of ion beam [33,34]. Similar set of experiment was performed for cross-shaped patterns as shown in Fig. 5b. At the fluence of 5.9×10^{11} ions/cm^2, the cross-shapes of the bitmap file were directly reflected on the PDMS surface, but no wrinkles were formed. By increasing the fluence, the ion-blanked regions in the bitmap file were affected due to ion beam broadening, which caused wrinkle-like structures near the irradiated region (middle plan) and the entire region by further increase in the fluence.

4. Conclusions

We provided a brief overview of a recent surface modification technique for polymers based on focused ion beam irradiation and highlighting the key advantages and limitations of the proposed technique. Moreover, some of the key experimental factors involved in patterning the polymeric surfaces by focused ion beam were examined. Specifically, we explored the role of pixel dwell time and ion fluence on the morphology of the created wrinkles. Long pixel dwell times leads to wrinkling patterns with distinct boundaries, while short pixel dwell time leads to non-uniform patterning of the surface with indistinct boundaries. Furthermore, ion beam shifting associated with fluence and the rastering number was explored by selecting the appropriate ion beam condition.

Acknowledgments

This research was supported in part by a grant from 'Center for Nanostructured Materials Technology' under '21st Century Frontier R&D Programs' of the Ministry of Science and Technology (code number: 06K1501-01613) (MWM, KRL), in part by the KOSEF grant funded by the Korea government, MOST, (No. R01-207-000-10032-0) (OKH, EKH), and in part by the support from NSF under grant CMMI-0736019 (AV).

References

[1] K. Efimenko, M. Rackaitis, E. Manias, A. Vaziri, L. Mahadevan, J. Genzer, Nat. Mater. 4 (2005) 1.
[2] J. El-Ali, P.K. Sorger, K.F. Jensen, Nature 442 (2006) 403.
[3] E.P. Chan, A.J. Crosby, Adv. Mater. 18 (2006) 3238.
[4] C. Harrison, C.M. Stafford, W. Zhang, A. Karim, Appl. Phys. Lett. 85 (2004) 4016.
[5] J. Genzer, J. Groenewold, Soft Matter 2 (2006) 310.
[6] G. Reiter, Phys. Rev. Lett. 68 (1992) 75.
[7] P.J. Yoo, K.Y. Suh, S.Y. Park, H.H. Lee, Adv. Mater. 14 (2002) 1383.

[8] N. Bowden, S. Brittain, A.G. Evans, J.W. Hutchinson, G.M. Whitesides, Nature 393 (1998) 146.
[9] S.P. Lacour, S.P.S. Wagner, Z. Huang, Z. Suo, Appl. Phys. Lett. 82 (2003) 2404.
[10] T. Ohzonoa, M. Shimomuraa, Phys. Rev., E 73 (2006) 040601.
[11] M.-W. Moon, S.H. Lee, J.-Y. Sun, K.H. Oh, A. Vaziri, J.W. Hutchinson, Proc. Natl Acad. Sci. U.S.A. 104 (2007) 1130.
[12] M.-W. Moon, S.H. Lee, J.-Y. Sun, K.H. Oh, A. Vaziri, J.W. Hutchinson, Scr. Mater. 57 (2007) 747.
[13] S. Klaumunzer, G. Schumacher, Phys. Rev. Lett. 51 (1983) 1987.
[14] E. Snoeks, T. Weber, A. Cacciato, A. Polman, J. Appl. Phys. 78 (1995) 4723.
[15] H. Dong, T. bell, Surf. Coat. Technol. 111 (1999) 29.
[16] K. Otani, X. Chen, J.W. Hutchinson, J.F. Chervinsky, M.J. Aziz, J. Appl. Phys. 100 (2006) 023535.
[17] Y.R. Kim, P. Chen, M.J. Aziz, D. Branton, J.J. Vlassak, J. Appl. Phys. 100 (2006) 104322.
[18] M. Ouyang, C. Yuan, R.J. Muisener, A. Boulares, J.T. Koberstein, Chem. Mater. 12 (2000) 1591.
[19] K. Efimenko, W.E. Wallace, J. Genzer, J. Colloid Interface Sci. 254 (2002) 306.
[20] A. Qureshi, N.L. Singh, A.K. Rakshit, F. Singh, D.K. Avasthi, Surf. Coat. Technol. 201 (2007) 8308.
[21] S. Klaumunzer, M.D. Hou, G. Schumacher, Phys. Rev. Lett. 57 (1986) 850.
[22] P. Sigmund, Phys. Rev. 184 (1969) 383.
[23] P. Sigmund, J. Mater. Sci. 8 (1973) 1545.
[24] R.M. Bradley, J.M. Harper, J. Vac. Sci. Technol., A 6 (1988) 2390.
[25] Y.-R. Kim, P. Chen, J.J. Aziz, D. Branton, J.J. Vlassak, J. Appl. Phys. 100 (2006) 104322.
[26] D.P. Adams, M.J. Vasile, J. Vac. Sci. Technol., B 24 (2006) 836.
[27] J. Erlebacher, M. Aziz, E. Chason, M. Sinclair, J. Floro, Phys. Rev. Lett. 82 (1999) 2330.
[28] J. Erlebacher, M.J. Aziz, E. Chason, M. Sinclair, J. Floro, Phys. Rev. Lett. 82 (1999) 2330.
[29] S. Facsko, T. Dekorsy, C. Koerdt, C. Trappe, H. Kurz, A. Vogt, H.L. Hartnagel, Science 285 (1999) 1551.
[30] M.-W. Moon, J.H. Han, A. Vaziri, E.K. Her, K.H. Oh, K.-R. Lee, J.W. Hutchinson, submitted for publication.
[31] S. Mandl, B. Rauschenbach, Surf. Coat. Technol. 156 (2002) 276.
[32] Y.J. Choi, M.S. Kim, I. Noh, Surf. Coat. Technol 201 (2007) 5724.
[33] Y. Fu, N.K.A. Bryan, O.N. Shing, H.N.P. Wyan, Sens. Actuators, A, Phys. 79 (2000) 230.
[34] W.C.L. Hopman, F. Ay, W. Hu, V.J. Gadgil, L. Kuipers, M. Pollnau, RR.M. de Ridder, Nanotechnology 18 (2007) 195305.
[35] X. Chen, J.W. Hutchinson, ASME J. Appl. Mech. 71 (2004) 597.
[36] J. Cazaux, J. Electron Spectrosc. Relat. Phenom. 105 (1999) 155.
[37] D. Briggs, A.B. Wootton, Surf. Interface Anal. 4 (1982) 109.